

Search for $\eta_c(2S) \rightarrow p\bar{p}K^+K^-$ and measurement of $\chi_{cJ} \rightarrow p\bar{p}K^+K^-$ in $\psi(3686)$ radiative decays

M. Ablikim¹, M. N. Achasov^{4,c}, P. Adlarson⁷⁶, O. Afedulidis³, X. C. Ai⁸¹, R. Aliberti³⁵, A. Amoroso^{75A,75C}, Y. Bai⁵⁷, O. Bakina³⁶, I. Balossino^{29A}, Y. Ban^{46,h}, H.-R. Bao⁶⁴, V. Batzskaya^{1,44}, K. Begzsuren³², N. Berger³⁵, M. Berlowski⁴⁴, M. Bertani^{28A}, D. Bettoni^{29A}, F. Bianchi^{75A,75C}, E. Bianco^{75A,75C}, A. Bortone^{75A,75C}, I. Boyko³⁶, R. A. Briere⁵, A. Brueggemann⁶⁹, H. Cai⁷⁷, X. Cai^{1,58}, A. Calcaterra^{28A}, G. F. Cao^{1,64}, N. Cao^{1,64}, S. A. Cetin^{62A}, X. Y. Chai^{46,h}, J. F. Chang^{1,58}, G. R. Che⁴³, Y. Z. Che^{1,58,64}, G. Chelkov^{36,b}, C. Chen⁴³, C. H. Chen⁹, Chao Chen⁵⁵, G. Chen¹, H. S. Chen^{1,64}, H. Y. Chen²⁰, M. L. Chen^{1,58,64}, S. J. Chen⁴², S. L. Chen⁴⁵, S. M. Chen⁶¹, T. Chen^{1,64}, X. R. Chen^{31,64}, X. T. Chen^{1,64}, Y. B. Chen^{1,58}, Y. Q. Chen³⁴, Z. J. Chen^{25,i}, S. K. Choi¹⁰, G. Cibinetto^{29A}, F. Cossio^{75C}, J. J. Cui⁵⁰, H. L. Dai^{1,58}, J. P. Dai⁷⁹, A. Dbeyssi¹⁸, R. E. de Boer³, D. Dedovich³⁶, C. Q. Deng⁷³, Z. Y. Deng¹, A. Denig³⁵, I. Denysenko³⁶, M. Destefanis^{75A,75C}, F. De Mori^{75A,75C}, B. Ding^{67,1}, X. X. Ding^{46,h}, Y. Ding³⁴, Y. Ding⁴⁰, J. Dong^{1,58}, L. Y. Dong^{1,64}, M. Y. Dong^{1,58,64}, X. Dong⁷⁷, M. C. Du¹, S. X. Du⁸¹, Y. Y. Duan⁵⁵, Z. H. Duan⁴², P. Egorov^{36,b}, G. F. Fan⁴², J. J. Fan¹⁹, Y. H. Fan⁴⁵, J. Fang⁵⁹, J. Fang^{1,58}, S. S. Fang^{1,64}, W. X. Fang¹, Y. Q. Fang^{1,58}, R. Farinelli^{29A}, L. Fava^{75B,75C}, F. Feldbauer³, G. Felici^{28A}, C. Q. Feng^{72,58}, J. H. Feng⁵⁹, Y. T. Feng^{72,58}, M. Fritsch³, C. D. Fu¹, J. L. Fu⁶⁴, Y. W. Fu^{1,64}, H. Gao⁶⁴, X. B. Gao⁴¹, Y. N. Gao^{46,h}, Y. N. Gao¹⁹, Yang Gao^{72,58}, S. Garbolino^{75C}, I. Garzia^{29A,29B}, P. T. Ge¹⁹, Z. W. Ge⁴², C. Geng⁵⁹, E. M. Gersabeck⁶⁸, A. Gilman⁷⁰, K. Goetzen¹³, L. Gong⁴⁰, W. X. Gong^{1,58}, W. Gradl³⁵, S. Gramigna^{29A,29B}, M. Greco^{75A,75C}, M. H. Gu^{1,58}, Y. T. Gu¹⁵, C. Y. Guan^{1,64}, A. Q. Guo^{31,64}, L. B. Guo⁴¹, M. J. Guo⁵⁰, R. P. Guo⁴⁹, Y. P. Guo^{12,g}, A. Guskov^{36,b}, J. Gutierrez²⁷, K. L. Han⁶⁴, T. T. Han¹, F. Hanisch³, X. Q. Hao¹⁹, F. A. Harris⁶⁶, K. K. He⁵⁵, K. L. He^{1,64}, F. H. Heinsius³, C. H. Heinz³⁵, Y. K. Heng^{1,58,64}, C. Herold⁶⁰, T. Holtmann³, P. C. Hong³⁴, G. Y. Hou^{1,64}, X. T. Hou^{1,64}, Y. R. Hou⁶⁴, Z. L. Hou¹, B. Y. Hu⁵⁹, H. M. Hu^{1,64}, J. F. Hu^{56,j}, Q. P. Hu^{72,58}, S. L. Hu^{12,g}, T. Hu^{1,58,64}, Y. Hu¹, G. S. Huang^{72,58}, K. X. Huang⁵⁹, L. Q. Huang^{31,64}, P. Huang⁴², X. T. Huang⁵⁰, Y. P. Huang¹, Y. S. Huang⁵⁹, T. Hussain⁷⁴, F. Hölzken³, N. Hüskens³⁵, N. in der Wiesche⁶⁹, J. Jackson²⁷, S. Janchiv³², Q. Ji¹, Q. P. Ji¹⁹, W. Ji^{1,64}, X. B. Ji^{1,64}, X. L. Ji^{1,58}, Y. Y. Ji⁵⁰, X. Q. Jia⁵⁰, Z. K. Jia^{72,58}, D. Jiang^{1,64}, H. B. Jiang⁷⁷, P. C. Jiang^{46,h}, S. S. Jiang³⁹, T. J. Jiang¹⁶, X. S. Jiang^{1,58,64}, Y. Jiang⁶⁴, J. B. Jiao⁵⁰, J. K. Jiao³⁴, Z. Jiao²³, S. Jin⁴², Y. Jin⁶⁷, M. Q. Jing^{1,64}, X. M. Jing⁶⁴, T. Johansson⁷⁶, S. Kabana³³, N. Kalantar-Nayestanaki⁶⁵, X. L. Kang⁹, X. S. Kang⁴⁰, M. Kavatsyuk⁶⁵, B. C. Ke⁸¹, V. Khachatryan²⁷, A. Khoukaz⁶⁹, R. Kiuchi¹, O. B. Kolcu^{62A}, B. Kopf³, M. Kuessner³, X. Kui^{1,64}, N. Kumar²⁶, A. Kupsc^{44,76}, W. Kühn³⁷, W. N. Lan¹⁹, T. T. Lei^{72,58}, Z. H. Lei^{72,58}, M. Lellmann³⁵, T. Lenz³⁵, C. Li⁴⁷, C. Li⁴³, C. H. Li³⁹, Cheng Li^{72,58}, D. M. Li⁸¹, F. Li^{1,58}, G. Li¹, H. B. Li^{1,64}, H. J. Li¹⁹, H. N. Li^{56,j}, Hui Li⁴³, J. R. Li⁶¹, J. S. Li⁵⁹, K. Li¹, K. L. Li¹⁹, L. J. Li^{1,64}, Lei Li⁴⁸, M. H. Li⁴³, P. L. Li⁶⁴, P. R. Li^{38,k,l}, Q. M. Li^{1,64}, Q. X. Li⁵⁰, R. Li^{17,31}, T. Li⁵⁰, T. Y. Li⁴³, W. D. Li^{1,64}, W. G. Li^{1,a}, X. Li^{1,64}, X. H. Li^{72,58}, X. L. Li⁵⁰, X. Y. Li^{1,8}, X. Z. Li⁵⁹, Y. Li¹⁹, Y. G. Li^{46,h}, Z. J. Li⁵⁹, Z. Y. Li⁷⁹, C. Liang⁴², H. Liang^{72,58}, Y. F. Liang⁵⁴, Y. T. Liang^{31,64}, G. R. Liao¹⁴, Y. P. Liao^{1,64}, J. Libby²⁶, A. Limphirat⁶⁰, C. C. Lin⁵⁵, C. X. Lin⁶⁴, D. X. Lin^{31,64}, T. Lin¹, B. J. Liu¹, B. X. Liu⁷⁷, C. Liu³⁴, C. X. Liu¹, F. Liu¹, F. H. Liu⁵³, Feng Liu⁶, G. M. Liu^{56,j}, H. Liu^{38,k,l}, H. B. Liu¹⁵, H. H. Liu¹, H. M. Liu^{1,64}, Huihui Liu²¹, J. B. Liu^{72,58}, K. Liu^{38,k,l}, K. Y. Liu⁴⁰, Ke Liu²², L. Liu^{72,58}, L. C. Liu⁴³, Lu Liu⁴³, M. H. Liu^{12,g}, P. L. Liu¹, Q. Liu⁶⁴, S. B. Liu^{72,58}, T. Liu^{12,g}, W. K. Liu⁴³, W. M. Liu^{72,58}, X. Liu³⁹, X. Liu^{38,k,l}, Y. Liu⁸¹, Y. Liu^{38,k,l}, Y. B. Liu⁴³, Z. A. Liu^{1,58,64}, Z. D. Liu⁹, Z. Q. Liu⁵⁰, X. C. Lou^{1,58,64}, F. X. Lu⁵⁹, H. J. Lu²³, J. G. Lu^{1,58}, Y. Lu⁷, Y. P. Lu^{1,58}, Z. H. Lu^{1,64}, C. L. Luo⁴¹, J. R. Luo⁵⁹, M. X. Luo⁸⁰, T. Luo^{12,g}, X. L. Luo^{1,58}, X. R. Lyu⁶⁴, Y. F. Lyu⁴³, F. C. Ma⁴⁰, H. Ma⁷⁹, H. L. Ma¹, J. L. Ma^{1,64}, L. L. Ma⁵⁰, L. R. Ma⁶⁷, Q. M. Ma¹, R. Q. Ma^{1,64}, R. Y. Ma¹⁹, T. Ma^{72,58}, X. T. Ma^{1,64}, X. Y. Ma^{1,58}, Y. M. Ma³¹, F. E. Maas¹⁸, I. MacKay⁷⁰, M. Maggiora^{75A,75C}, S. Malde⁷⁰, Y. J. Mao^{46,h}, Z. P. Mao¹, S. Marcello^{75A,75C}, Y. H. Meng⁶⁴, Z. X. Meng⁶⁷, J. G. Messchendorp^{13,65}, G. Mezzadri^{29A}, H. Miao^{1,64}, T. J. Min⁴², R. E. Mitchell²⁷, X. H. Mo^{1,58,64}, B. Moses²⁷, N. Yu. Muchnoi^{4,c}, J. Muskalla³⁵, Y. Nefedov³⁶, F. Nerling^{18,e}, L. S. Nie²⁰, I. B. Nikolaev^{4,c}, Z. Ning^{1,58}, S. Nisar^{11,m}, Q. L. Niu^{38,k,l}, W. D. Niu⁵⁵, Y. Niu⁵⁰, S. L. Olsen^{10,64}, Q. Ouyang^{1,58,64}, S. Pacetti^{28B,28C}, X. Pan⁵⁵, Y. Pan⁵⁷, A. Pathak¹⁰, Y. P. Pei^{72,58}, M. Pelizaeus³, H. P. Peng^{72,58}, Y. Y. Peng^{38,k,l}, K. Peters^{13,e}, J. L. Ping⁴¹, R. G. Ping^{1,64}, S. Plura³⁵, V. Prasad³³, F. Z. Qi¹, H. R. Qi⁶¹, M. Qi⁴², S. Qian^{1,58}, W. B. Qian⁶⁴, C. F. Qiao⁶⁴, J. H. Qiao¹⁹, J. J. Qin⁷³, L. Q. Qin¹⁴, L. Y. Qin^{72,58}, X. P. Qin^{12,g}, X. S. Qin⁵⁰, Z. H. Qin^{1,58}, J. F. Qiu¹, Z. H. Qu⁷³, C. F. Redmer³⁵, K. J. Ren³⁹, A. Rivetti^{75C}, M. Rolo^{75C}, G. Rong^{1,64}, Ch. Rosner¹⁸, M. Q. Ruan^{1,58}, S. N. Ruan⁴³, N. Salone⁴⁴, A. Sarantsev^{36,d}, Y. Schelhaas³⁵, K. Schoenning⁷⁶, M. Scodreggio^{29A}, K. Y. Shan^{12,g}, W. Shan²⁴, X. Y. Shan^{72,58}, Z. J. Shang^{38,k,l}, J. F. Shanguan¹⁶, L. G. Shao^{1,64}, M. Shao^{72,58}, C. P. Shen^{12,g}, H. F. Shen^{1,8}, W. H. Shen⁶⁴, X. Y. Shen^{1,64}, B. A. Shi⁶⁴, H. Shi^{72,58}, J. L. Shi^{12,g}, J. Y. Shi¹, S. Y. Shi⁷³, X. Shi^{1,58},

J. J. Song¹⁹, T. Z. Song⁵⁹, W. M. Song^{34,1}, Y. J. Song^{12,g}, Y. X. Song^{46,h,n}, S. Sosio^{75A,75C}, S. Spataro^{75A,75C}, F. Stieler³⁵, S. S. Su⁴⁰, Y. J. Su⁶⁴, G. B. Sun⁷⁷, G. X. Sun¹, H. Sun⁶⁴, H. K. Sun¹, J. F. Sun¹⁹, K. Sun⁶¹, L. Sun⁷⁷, S. S. Sun^{1,64}, T. Sun^{51,f}, Y. J. Sun^{72,58}, Y. Z. Sun¹, Z. Q. Sun^{1,64}, Z. T. Sun⁵⁰, C. J. Tang⁵⁴, G. Y. Tang¹, J. Tang⁵⁹, M. Tang^{72,58}, Y. A. Tang⁷⁷, L. Y. Tao⁷³, M. Tat⁷⁰, J. X. Teng^{72,58}, V. Thoren⁷⁶, W. H. Tian⁵⁹, Y. Tian^{31,64}, Z. F. Tian⁷⁷, I. Uman^{62B}, Y. Wan⁵⁵, S. J. Wang⁵⁰, B. Wang¹, Bo Wang^{72,58}, C. Wang¹⁹, D. Y. Wang^{46,h}, H. J. Wang^{38,k,l}, J. J. Wang⁷⁷, J. P. Wang⁵⁰, K. Wang^{1,58}, L. L. Wang¹, L. W. Wang³⁴, M. Wang⁵⁰, N. Y. Wang⁶⁴, S. Wang^{12,g}, S. Wang^{38,k,l}, T. Wang^{12,g}, T. J. Wang⁴³, W. Wang⁵⁹, W. Wang⁷³, W. P. Wang^{35,58,72,o}, X. Wang^{46,h}, X. F. Wang^{38,k,l}, X. J. Wang³⁹, X. L. Wang^{12,g}, X. N. Wang¹, Y. Wang⁶¹, Y. D. Wang⁴⁵, Y. F. Wang^{1,58,64}, Y. H. Wang^{38,k,l}, Y. L. Wang¹⁹, Y. N. Wang⁴⁵, Y. Q. Wang¹, Yaqian Wang¹⁷, Yi Wang⁶¹, Z. Wang^{1,58}, Z. L. Wang⁷³, Z. Y. Wang^{1,64}, D. H. Wei¹⁴, F. Weidner⁶⁹, S. P. Wen¹, Y. R. Wen³⁹, U. Wiedner³, G. Wilkinson⁷⁰, M. Wolke⁷⁶, L. Wollenberg³, C. Wu³⁹, J. F. Wu^{1,8}, L. H. Wu¹, L. J. Wu^{1,64}, Lianjie Wu¹⁹, X. Wu^{12,g}, X. H. Wu³⁴, Y. H. Wu⁵⁵, Y. J. Wu³¹, Z. Wu^{1,58}, L. Xia^{72,58}, X. M. Xian³⁹, B. H. Xiang^{1,64}, T. Xiang^{46,h}, D. Xiao^{38,k,l}, G. Y. Xiao⁴², H. Xiao⁷³, Y. L. Xiao^{12,g}, Z. J. Xiao⁴¹, C. Xie⁴², X. H. Xie^{46,h}, Y. Xie⁵⁰, Y. G. Xie^{1,58}, Y. H. Xie⁶, Z. P. Xie^{72,58}, T. Y. Xing^{1,64}, C. F. Xu^{1,64}, C. J. Xu⁵⁹, G. F. Xu¹, M. Xu^{72,58}, Q. J. Xu¹⁶, Q. N. Xu³⁰, W. L. Xu⁶⁷, X. P. Xu⁵⁵, Y. Xu⁴⁰, Y. C. Xu⁷⁸, Z. S. Xu⁶⁴, F. Yan^{12,g}, L. Yan^{12,g}, W. B. Yan^{72,58}, W. C. Yan⁸¹, W. P. Yan¹⁹, X. Q. Yan^{1,64}, H. J. Yang^{51,f}, H. L. Yang³⁴, H. X. Yang¹, J. H. Yang⁴², R. J. Yang¹⁹, T. Yang¹, Y. Yang^{12,g}, Y. F. Yang⁴³, Y. X. Yang^{1,64}, Y. Z. Yang¹⁹, Z. W. Yang^{38,k,l}, Z. P. Yao⁵⁰, M. Ye^{1,58}, M. H. Ye⁸, Junhao Yin⁴³, Z. Y. You⁵⁹, B. X. Yu^{1,58,64}, C. X. Yu⁴³, G. Yu¹³, J. S. Yu^{25,i}, M. C. Yu⁴⁰, T. Yu⁷³, X. D. Yu^{46,h}, C. Z. Yuan^{1,64}, J. Yuan³⁴, J. Yuan⁴⁵, L. Yuan², S. C. Yuan^{1,64}, Y. Yuan^{1,64}, Z. Y. Yuan⁵⁹, C. X. Yue³⁹, Ying Yue¹⁹, A. A. Zafar⁷⁴, F. R. Zeng⁵⁰, S. H. Zeng^{63A,63B,63C,63D}, X. Zeng^{12,g}, Y. Zeng^{25,i}, Y. J. Zeng⁵⁹, Y. J. Zeng^{1,64}, X. Y. Zhai³⁴, Y. C. Zhai⁵⁰, Y. H. Zhan⁵⁹, A. Q. Zhang^{1,64}, B. L. Zhang^{1,64}, B. X. Zhang¹, D. H. Zhang⁴³, G. Y. Zhang¹⁹, H. Zhang⁸¹, H. Zhang^{72,58}, H. C. Zhang^{1,58,64}, H. H. Zhang⁵⁹, H. Q. Zhang^{1,58,64}, H. R. Zhang^{72,58}, H. Y. Zhang^{1,58}, J. Zhang⁵⁹, J. Zhang⁸¹, J. J. Zhang⁵², J. L. Zhang²⁰, J. Q. Zhang⁴¹, J. S. Zhang^{12,g}, J. W. Zhang^{1,58,64}, J. X. Zhang^{38,k,l}, J. Y. Zhang¹, J. Z. Zhang^{1,64}, Jianyu Zhang⁶⁴, L. M. Zhang⁶¹, Lei Zhang⁴², P. Zhang^{1,64}, Q. Zhang¹⁹, Q. Y. Zhang³⁴, R. Y. Zhang^{38,k,l}, S. H. Zhang^{1,64}, Shulei Zhang^{25,i}, X. M. Zhang¹, X. Y. Zhang⁴⁰, X. Y. Zhang⁵⁰, Y. Zhang⁷³, Y. Zhang¹, Y. T. Zhang⁸¹, Y. H. Zhang^{1,58}, Y. M. Zhang³⁹, Yan Zhang^{72,58}, Z. D. Zhang¹, Z. H. Zhang¹, Z. L. Zhang³⁴, Z. X. Zhang¹⁹, Z. Y. Zhang⁴³, Z. Y. Zhang⁷⁷, Z. Z. Zhang⁴⁵, Zh. Zh. Zhang¹⁹, G. Zhao¹, J. Y. Zhao^{1,64}, J. Z. Zhao^{1,58}, L. Zhao¹, Lei Zhao^{72,58}, M. G. Zhao⁴³, N. Zhao⁷⁹, R. P. Zhao⁶⁴, S. J. Zhao⁸¹, Y. B. Zhao^{1,58}, Y. X. Zhao^{31,64}, Z. G. Zhao^{72,58}, A. Zhemchugov^{36,b}, B. Zheng⁷³, B. M. Zheng³⁴, J. P. Zheng^{1,58}, W. J. Zheng^{1,64}, X. R. Zheng¹⁹, Y. H. Zheng⁶⁴, B. Zhong⁴¹, X. Zhong⁵⁹, H. Zhou^{35,50,o}, J. Y. Zhou³⁴, S. Zhou⁶, X. Zhou⁷⁷, X. K. Zhou⁶, X. R. Zhou^{72,58}, X. Y. Zhou³⁹, Y. Z. Zhou^{12,g}, Z. C. Zhou²⁰, A. N. Zhu⁶⁴, J. Zhu⁴³, K. Zhu¹, K. J. Zhu^{1,58,64}, K. S. Zhu^{12,g}, L. Zhu³⁴, L. X. Zhu⁶⁴, S. H. Zhu⁷¹, T. J. Zhu^{12,g}, W. D. Zhu⁴¹, W. Z. Zhu¹⁹, Y. C. Zhu^{72,58}, Z. A. Zhu^{1,64}, J. H. Zou¹, J. Zu^{72,58}

(BESIII Collaboration)

¹ *Institute of High Energy Physics, Beijing 100049, People's Republic of China*

² *Beihang University, Beijing 100191, People's Republic of China*

³ *Bochum Ruhr-University, D-44780 Bochum, Germany*

⁴ *Budker Institute of Nuclear Physics SB RAS (BINP), Novosibirsk 630090, Russia*

⁵ *Carnegie Mellon University, Pittsburgh, Pennsylvania 15213, USA*

⁶ *Central China Normal University, Wuhan 430079, People's Republic of China*

⁷ *Central South University, Changsha 410083, People's Republic of China*

⁸ *China Center of Advanced Science and Technology, Beijing 100190, People's Republic of China*

⁹ *China University of Geosciences, Wuhan 430074, People's Republic of China*

¹⁰ *Chung-Ang University, Seoul, 06974, Republic of Korea*

¹¹ *COMSATS University Islamabad, Lahore Campus, Defence Road, Off Raiwind Road, 54000 Lahore, Pakistan*

¹² *Fudan University, Shanghai 200433, People's Republic of China*

¹³ *GSI Helmholtzcentre for Heavy Ion Research GmbH, D-64291 Darmstadt, Germany*

¹⁴ *Guangxi Normal University, Guilin 541004, People's Republic of China*

¹⁵ *Guangxi University, Nanning 530004, People's Republic of China*

¹⁶ *Hangzhou Normal University, Hangzhou 310036, People's Republic of China*

¹⁷ *Hebei University, Baoding 071002, People's Republic of China*

¹⁸ *Helmholtz Institute Mainz, Staudinger Weg 18, D-55099 Mainz, Germany*

¹⁹ *Henan Normal University, Xinxiang 453007, People's Republic of China*

- ²⁰ Henan University, Kaifeng 475004, People's Republic of China
- ²¹ Henan University of Science and Technology, Luoyang 471003, People's Republic of China
- ²² Henan University of Technology, Zhengzhou 450001, People's Republic of China
- ²³ Huangshan College, Huangshan 245000, People's Republic of China
- ²⁴ Hunan Normal University, Changsha 410081, People's Republic of China
- ²⁵ Hunan University, Changsha 410082, People's Republic of China
- ²⁶ Indian Institute of Technology Madras, Chennai 600036, India
- ²⁷ Indiana University, Bloomington, Indiana 47405, USA
- ²⁸ INFN Laboratori Nazionali di Frascati, (A)INFN Laboratori Nazionali di Frascati, I-00044, Frascati, Italy; (B)INFN Sezione di Perugia, I-06100, Perugia, Italy; (C)University of Perugia, I-06100, Perugia, Italy
- ²⁹ INFN Sezione di Ferrara, (A)INFN Sezione di Ferrara, I-44122, Ferrara, Italy; (B)University of Ferrara, I-44122, Ferrara, Italy
- ³⁰ Inner Mongolia University, Hohhot 010021, People's Republic of China
- ³¹ Institute of Modern Physics, Lanzhou 730000, People's Republic of China
- ³² Institute of Physics and Technology, Peace Avenue 54B, Ulaanbaatar 13330, Mongolia
- ³³ Instituto de Alta Investigación, Universidad de Tarapacá, Casilla 7D, Arica 1000000, Chile
- ³⁴ Jilin University, Changchun 130012, People's Republic of China
- ³⁵ Johannes Gutenberg University of Mainz, Johann-Joachim-Becher-Weg 45, D-55099 Mainz, Germany
- ³⁶ Joint Institute for Nuclear Research, 141980 Dubna, Moscow region, Russia
- ³⁷ Justus-Liebig-Universität Giessen, II. Physikalisches Institut, Heinrich-Buff-Ring 16, D-35392 Giessen, Germany
- ³⁸ Lanzhou University, Lanzhou 730000, People's Republic of China
- ³⁹ Liaoning Normal University, Dalian 116029, People's Republic of China
- ⁴⁰ Liaoning University, Shenyang 110036, People's Republic of China
- ⁴¹ Nanjing Normal University, Nanjing 210023, People's Republic of China
- ⁴² Nanjing University, Nanjing 210093, People's Republic of China
- ⁴³ Nankai University, Tianjin 300071, People's Republic of China
- ⁴⁴ National Centre for Nuclear Research, Warsaw 02-093, Poland
- ⁴⁵ North China Electric Power University, Beijing 102206, People's Republic of China
- ⁴⁶ Peking University, Beijing 100871, People's Republic of China
- ⁴⁷ Qufu Normal University, Qufu 273165, People's Republic of China
- ⁴⁸ Renmin University of China, Beijing 100872, People's Republic of China
- ⁴⁹ Shandong Normal University, Jinan 250014, People's Republic of China
- ⁵⁰ Shandong University, Jinan 250100, People's Republic of China
- ⁵¹ Shanghai Jiao Tong University, Shanghai 200240, People's Republic of China
- ⁵² Shanxi Normal University, Linfen 041004, People's Republic of China
- ⁵³ Shanxi University, Taiyuan 030006, People's Republic of China
- ⁵⁴ Sichuan University, Chengdu 610064, People's Republic of China
- ⁵⁵ Soochow University, Suzhou 215006, People's Republic of China
- ⁵⁶ South China Normal University, Guangzhou 510006, People's Republic of China
- ⁵⁷ Southeast University, Nanjing 211100, People's Republic of China
- ⁵⁸ State Key Laboratory of Particle Detection and Electronics, Beijing 100049, Hefei 230026, People's Republic of China
- ⁵⁹ Sun Yat-Sen University, Guangzhou 510275, People's Republic of China
- ⁶⁰ Suranaree University of Technology, University Avenue 111, Nakhon Ratchasima 30000, Thailand
- ⁶¹ Tsinghua University, Beijing 100084, People's Republic of China
- ⁶² Turkish Accelerator Center Particle Factory Group, (A)Istinye University, 34010, Istanbul, Turkey; (B)Near East University, Nicosia, North Cyprus, 99138, Mersin 10, Turkey
- ⁶³ University of Bristol, H H Wills Physics Laboratory, Tyndall Avenue, Bristol, BS8 1TL, UK
- ⁶⁴ University of Chinese Academy of Sciences, Beijing 100049, People's Republic of China
- ⁶⁵ University of Groningen, NL-9747 AA Groningen, The Netherlands
- ⁶⁶ University of Hawaii, Honolulu, Hawaii 96822, USA
- ⁶⁷ University of Jinan, Jinan 250022, People's Republic of China
- ⁶⁸ University of Manchester, Oxford Road, Manchester, M13 9PL, United Kingdom

⁶⁹ *University of Muenster, Wilhelm-Klemm-Strasse 9, 48149 Muenster, Germany*

⁷⁰ *University of Oxford, Keble Road, Oxford OX13RH, United Kingdom*

⁷¹ *University of Science and Technology Liaoning, Anshan 114051, People's Republic of China*

⁷² *University of Science and Technology of China, Hefei 230026, People's Republic of China*

⁷³ *University of South China, Hengyang 421001, People's Republic of China*

⁷⁴ *University of the Punjab, Lahore-54590, Pakistan*

⁷⁵ *University of Turin and INFN, (A)University of Turin, I-10125, Turin, Italy; (B)University of Eastern Piedmont, I-15121, Alessandria, Italy; (C)INFN, I-10125, Turin, Italy*

⁷⁶ *Uppsala University, Box 516, SE-75120 Uppsala, Sweden*

⁷⁷ *Wuhan University, Wuhan 430072, People's Republic of China*

⁷⁸ *Yantai University, Yantai 264005, People's Republic of China*

⁷⁹ *Yunnan University, Kunming 650500, People's Republic of China*

⁸⁰ *Zhejiang University, Hangzhou 310027, People's Republic of China*

⁸¹ *Zhengzhou University, Zhengzhou 450001, People's Republic of China*

^a *Deceased*

^b *Also at the Moscow Institute of Physics and Technology, Moscow 141700, Russia*

^c *Also at the Novosibirsk State University, Novosibirsk, 630090, Russia*

^d *Also at the NRC "Kurchatov Institute", PNPI, 188300, Gatchina, Russia*

^e *Also at Goethe University Frankfurt, 60323 Frankfurt am Main, Germany*

^f *Also at Key Laboratory for Particle Physics, Astrophysics and Cosmology, Ministry of Education; Shanghai Key Laboratory for Particle Physics and Cosmology; Institute of Nuclear and Particle Physics, Shanghai 200240, People's Republic of China*

^g *Also at Key Laboratory of Nuclear Physics and Ion-beam Application (MOE) and Institute of Modern Physics, Fudan University, Shanghai 200443, People's Republic of China*

^h *Also at State Key Laboratory of Nuclear Physics and Technology, Peking University, Beijing 100871, People's Republic of China*

ⁱ *Also at School of Physics and Electronics, Hunan University, Changsha 410082, China*

^j *Also at Guangdong Provincial Key Laboratory of Nuclear Science, Institute of Quantum Matter, South China Normal University, Guangzhou 510006, China*

^k *Also at MOE Frontiers Science Center for Rare Isotopes, Lanzhou University, Lanzhou 730000, People's Republic of China*

^l *Also at Lanzhou Center for Theoretical Physics, Lanzhou University, Lanzhou 730000, People's Republic of China*

^m *Also at the Department of Mathematical Sciences, IBA, Karachi 75270, Pakistan*

ⁿ *Also at Ecole Polytechnique Federale de Lausanne (EPFL), CH-1015 Lausanne, Switzerland*

^o *Also at Helmholtz Institute Mainz, Staudinger Weg 18, D-55099 Mainz, Germany*

A search for $\eta_c(2S) \rightarrow p\bar{p}K^+K^-$, together with measurement of branching fractions of $\chi_{cJ}(J=0,1,2) \rightarrow p\bar{p}K^+K^-$ in the $\psi(3686) \rightarrow \gamma\eta_c(2S)$ and the $\psi(3686) \rightarrow \gamma\chi_{cJ}$ radiative decays, is performed with $(2712.4 \pm 14.3) \times 10^6$ $\psi(3686)$ events collected with the BESIII detector at the BEPCII collider. An evidence for $\eta_c(2S) \rightarrow p\bar{p}K^+K^-$ is found, with a significance of 3.3σ . The product branching fraction of $\mathcal{B}[\psi(3686) \rightarrow \gamma\eta_c(2S)] \cdot \mathcal{B}[\eta_c(2S) \rightarrow p\bar{p}K^+K^-]$ is determined to be $(1.98 \pm 0.41_{\text{stat.}} \pm 0.99_{\text{syst.}}) \times 10^{-7}$. The product branching fractions of $\mathcal{B}[\psi(3686) \rightarrow \gamma\chi_{cJ}] \cdot \mathcal{B}[\chi_{cJ} \rightarrow p\bar{p}K^+K^-]$ are measured to be $(2.49 \pm 0.03_{\text{stat.}} \pm 0.15_{\text{syst.}}) \times 10^{-5}$, $(1.83 \pm 0.02_{\text{stat.}} \pm 0.11_{\text{syst.}}) \times 10^{-5}$, and $(2.43 \pm 0.02_{\text{stat.}} \pm 0.15_{\text{syst.}}) \times 10^{-5}$, for $J = 0, 1$, and 2 , respectively.

I. INTRODUCTION

The charmonia below the open-charm threshold are well established, and their spectrum can be well described by the Quantum Chromodynamics (QCD) or QCD-inspired models. The study of these charmonia would offer valuable insights into QCD, and provide valuable reference for decoding the nature of many exotic candidates above the open-charm threshold. However,

the decay dynamics of the charmonia is far from being well understood.

The “ $\rho\pi$ puzzle” remains an outstanding issue for the vector charmonia [1]. The puzzle stems from the theoretical prediction that the ratio Q_V , defined by

$$Q_V = \frac{\mathcal{B}[\psi(3686) \rightarrow \text{hadrons}]}{\mathcal{B}[J/\psi \rightarrow \text{hadrons}]}, \quad (1)$$

should be about 12% [2]. This prediction is borne out by

many measurements of exclusive decay modes, but there are some anomalous results from the $\rho\pi$ and other decay modes [3]. A similar ratio is also proposed for pseudoscalar charmonia, denoted as Q_P ,

$$Q_P = \frac{\mathcal{B}[\eta_c(2S) \rightarrow \text{hadrons}]}{\mathcal{B}[\eta_c \rightarrow \text{hadrons}]}.$$
 (2)

Yet, the available expectation values for Q_P from different theories are inconsistent [4, 5].

By analyzing existing experimental data on pseudoscalar charmonium decays, a combined fit [6] is performed to retrieve Q_P . The result indicates that the fitted ratios from the experimental data are significantly different from both of the theoretical models [4, 5], and the branching fractions of almost all exclusive decay modes of $\eta_c(2S)$ are smaller than those of η_c . These discrepancies could hint at the intriguing decay dynamics of η_c and $\eta_c(2S)$.

Compared to J/ψ and $\psi(3686)$, the states of η_c and $\eta_c(2S)$ are relatively less studied, especially for the latter. The $\eta_c(2S)$ was first observed by Belle in B decays [7] in 2002, and was subsequently corroborated by BaBar and CLEO [8–10] in two-photon fusion reactions. The $\eta_c(2S)$ can also be produced in the magnetic dipole (M1) transition of $\psi(3686)$. Due to the small branching fraction of the M1 transition [11–15], a large $\psi(3686)$ sample is needed. Moreover, good performance of the electromagnetic calorimeter (EMC) is required to detect the low-energy M1 photon. It was not until 2012 that the $\eta_c(2S)$ from M1 transition of $\psi(3686)$ was firstly observed by BESIII in $\eta_c(2S) \rightarrow K_s^0 K^\pm \pi^\mp$ and $\eta_c(2S) \rightarrow K^+ K^- \pi^0$ decay modes [16], with a statistical significance greater than 10σ . So far, as compiled by the Particle Data Group (PDG), the measured branching fractions of $\eta_c(2S)$ only add up to roughly 7% [17]. Further investigations into its additional decay modes are needed.

In this paper, we perform a search for the $\eta_c(2S) \rightarrow p\bar{p}K^+K^-$ process in the radiative decay $\psi(3686) \rightarrow \gamma\eta_c(2S)$ with $(2712.4 \pm 14.3) \times 10^6$ $\psi(3686)$ events collected by BESIII in 2009, 2012, and 2021 [18]. The $\chi_{cJ}(J=0,1,2)$ states, the P -wave spin-triplet charmonia, have been observed to decay into the same final state with 106 million $\psi(3686)$ events [19]. The $\chi_{cJ} \rightarrow p\bar{p}K^+K^-$ are dominant backgrounds for $\eta_c(2S) \rightarrow p\bar{p}K^+K^-$, so improved measurements of these decays are important to extract a reliable yield of the $\eta_c(2S)$ decay. The product branching fractions of $\psi(3686) \rightarrow \gamma\chi_{cJ} \rightarrow \gamma p\bar{p}K^+K^-$ are measured for the first time in this paper.

II. BESIII DETECTOR AND MONTE CARLO SIMULATION

The BESIII detector at BEPCII is designed to study hadron spectroscopy and τ -charm physics [20]. The cylindrical BESIII is composed of a Helium-gas based multilayer drift chamber (MDC) with superconducting quadrupoles inserted in the conical shaped end caps, a

Time-of-Flight (TOF) system located outside the MDC, a CsI(Tl) EMC placed outside of the TOF system and inside the superconducting solenoid, providing 1.0 T magnetic field in the central region of BESIII, a muon identifier outside the superconducting solenoid consisting of layers of resistive plate chambers inserted in gaps between steel plates of the flux return yoke. The momentum resolution of charged particles at 1 GeV is 0.5% and the dE/dx resolution is 6% for the electrons from Bhabha scattering at 1 GeV. The photon energies are measured by the EMC with a resolution of 2.5% (5%) at 1 GeV in the barrel (end-cap) region. The time resolution of the barrel (end-cap) TOF system is 68 ps (110 ps). The end-cap TOF system was upgraded in 2015 using the multi-gap resistive plate chamber technology, improving the time resolution from 110 ps to 60 ps [21–23], which benefits 83% of the data used in this analysis.

Simulated Monte Carlo (MC) samples are produced by GEANT4-based simulation software BOOST [24, 25], which includes the geometric description of the BESIII detector, as well as the running conditions and response. The production of $\psi(3686)$ is simulated using KKMC [26, 27], and the hadronic decay of $\psi(3686)$ is generated by EVTGEN [28, 29] with branching fractions of known decay modes from PDG, or by LUNDCHARM for unobserved decay modes. The final state radiation (FSR) from charged particles is incorporated with the PHOTOS package [30].

To study the detection efficiencies, exclusive MC samples of $\psi(3686) \rightarrow \gamma\chi_{cJ}$, with χ_{cJ} decays to $p\bar{p}K^+K^-$ and $\chi_{cJ} \rightarrow I \rightarrow p\bar{p}K^+K^-$ are generated by the phase-space model, where I stands for intermediate states including $\Lambda(1520)\bar{\Lambda}(1520)$, $\Lambda(1520)\bar{p}K^+ + c.c.$, and $p\bar{p}\phi$. The efficiencies of $\psi(3686) \rightarrow \gamma\chi_{cJ} \rightarrow \gamma p\bar{p}K^+K^-$ are obtained from a synthesis MC sample in which these processes with different decay dynamics are mixed according to the branching fractions measured previously with the 106 million $\psi(3686)$ events [19]. An exclusive MC sample of $\psi(3686) \rightarrow \gamma\eta_c(2S) \rightarrow \gamma p\bar{p}K^+K^-$, where the $\eta_c(2S)$ decay is generated with the phase-space model, is used to estimate the efficiency of the $\eta_c(2S)$ decay signal. In the production processes of $\psi(3686) \rightarrow \gamma\chi_{cJ}$ and $\gamma\eta_c(2S)$, the photon follows the angular distribution of $1 + \alpha \cos^2 \theta_\gamma$, where θ_γ is the polar angle of the photon's momentum in the rest frame of e^+e^- . From the conservation of C and P parities, α is 1 for $\eta_c(2S)$. Assuming χ_{c0} and χ_{c1} are produced in electric dipole (E1) transition, α is 1 and $-1/3$ for χ_{c0} and χ_{c1} , respectively. Experimental measurements from Ref. [31] are used for χ_{c2} , from which the α is about $1/12$. An exclusive background MC sample of $\psi(3686) \rightarrow p\bar{p}K^+K^-$ and an inclusive MC sample comprising 2.747 billion $\psi(3686)$ events are utilized for background study. The inclusive MC sample includes the production of the $\psi(3686)$ resonance, the initial-state radiation production of the J/ψ meson, and the continuum processes incorporated in KKMC. The TOPOANA package [32] is used to analyze the decay chains of events in the inclusive MC sample.

III. EVENT SELECTION AND BACKGROUND ANALYSIS

Candidate events must have four charged tracks and at least one photon. Charged tracks in the MDC are required to satisfy $|\cos\theta| < 0.93$, where θ represents the polar angle with respect to the positron beam direction. Events with two oppositely charged track pairs are selected. The minimum distance of the closest points of the tracks to the interaction point is required to be less than 1 cm in the transverse plane and less than 10 cm in the beam direction. Particle identification (PID) is performed on each charged track, combining the TOF and dE/dx information. The PID hypothesis with the highest probability is assigned to the track, where we require a minimum PID confidence level (C.L.) of 0.1%. After the PID, we select events containing exactly one p , \bar{p} , K^+ , and K^- .

For identification of photon candidates, the deposited energy of each shower in the EMC must be larger than 25 MeV in the barrel region ($|\cos\theta| < 0.80$), and larger than 40 MeV in the end-cap region ($0.86 < |\cos\theta| < 0.92$). The interval between the EMC time and the event start time is required to be within $[0, 700]$ ns for noise suppression. A vertex fit is performed with the four charged tracks, and only events with successful vertex fits are retained. Then a kinematic fit with four constraints (4C) is performed to ensure energy-momentum conservation between the initial and final states. If there are multiple photon candidates, the one with the lowest χ_{4C}^2 value is selected as the photon emitted from $\psi(3686)$. A subsequent three-constraint (3C) kinematic fit is carried out, where the energy of the photon is free to vary. This 3C kinematic fit can provide a better separation of $\eta_c(2S)$ signal from the background.

The χ_{4C}^2 criterium is optimized by maximizing the figure of merit (FOM) given by

$$\text{FOM}_a = \frac{S}{\frac{b^2}{2} + a\sqrt{B} + \frac{b}{2}\sqrt{b^2 + 4a\sqrt{B} + 4B}}, \quad (3)$$

following the discussion in Ref. [33]. In Eq. (3), B is the number of background events in the χ_{c2} mass region ($[3.53, 3.58]$ GeV/ c^2), obtained from the inclusive MC sample. The symbol S represents the number of signal events in the same region, obtained using the exclusive MC sample of $\psi(3686) \rightarrow \gamma\chi_{c2} \rightarrow \gamma p\bar{p}K^+K^-$, normalized according to the branching fractions of $\chi_{c2} \rightarrow p\bar{p}K^+K^-$, $\chi_{c2} \rightarrow \Lambda(1520)\bar{p}K^+ + c.c.$, $\chi_{c2} \rightarrow \Lambda(1520)\bar{\Lambda}(1520)$, and $\chi_{c2} \rightarrow p\bar{p}\phi$ from the PDG. The parameter a represents the significance level, characterizing the probability of rejecting the null hypothesis when it is true, and b describes the confidence level, such that the value of $1 - \text{C.L.}$ is the probability of rejecting the alternative hypothesis. The optimization is stable for different combinations of a and b .

There is a discrepancy between the MC and data samples for the fake photons which denote photons not se-

lected by the 4C kinematic fit. This discrepancy manifests in the distribution of $\theta(\gamma, \bar{p}) - E_\gamma$, where E_γ is the energy of the fake photon and $\theta(\gamma, \bar{p})$ is the angle between the three-momentum of the fake photon and the \bar{p} . This discrepancy will affect the efficiency evaluated by the MC simulation. Using $\psi(3686) \rightarrow \gamma\chi_{c2} \rightarrow \gamma p\bar{p}K^+K^-$ as control sample, we compare the two dimensional distribution between the control sample and the corresponding MC sample. The $\theta(\gamma, \bar{p})$ is divided into bins with 10° width and E_γ is divided into bins with 25 MeV width. The ratio $r = n^{\text{Data}}/n^{\text{MC}}$ is calculated for each bin, where $n^{\text{Data(MC)}}$ is the number of fake photons in data (normalized MC sample) in one bin. The truth matching is performed to the photons before the 4C kinematic fit in all MC samples. Fake photons identified in the MC sample are re-sampled according to the ratio r to match the yields in data as a function of E_γ and $\theta(\gamma, \bar{p})$. The re-sampled photon candidates in the MC samples are then subject to the 4C kinematic fit. After this procedure, the $\theta(\gamma, \bar{p}) - E_\gamma$ distribution of fake photons in MC sample is consistent with that in the data, while other distributions like $\theta(\gamma, p)$, $\theta(\gamma, K^\pm)$ are not affected.

The study of the inclusive MC sample indicates the presence of background from the $\psi(3686) \rightarrow p\bar{p}K^+K^-$ process, where an FSR photon or a spurious photon from the detector is misidentified as the one directly from the $\psi(3686)$ radiation. In the invariant mass spectrum of $p\bar{p}K^+K^-$ from the 3C kinematic fit, this background peaks at the mass of $\psi(3686)$ and extends to 3.6 GeV. The lineshape of $\psi(3686) \rightarrow p\bar{p}K^+K^-$ depends on the fraction of FSR process f_{FSR} , defined as

$$f_{\text{FSR}} = \frac{N_{\text{FSR}}}{N_{\text{nonFSR}}}, \quad (4)$$

where the numerator and the denominator are the numbers of FSR and non-FSR event yields, respectively. The fraction f_{FSR} is usually different for the MC and data. Using the control sample of $\psi(3686) \rightarrow \gamma\chi_{c0} \rightarrow \gamma\gamma_{\text{FSR}}p\bar{p}K^+K^-$, the ratio $R_{\text{FSR}} = f_{\text{FSR}}^{\text{Data}}/f_{\text{FSR}}^{\text{MC}} = 2.38 \pm 0.90$ is determined, where the uncertainty is statistical only. The fraction of FSR events in the exclusive $\psi(3686) \rightarrow p\bar{p}K^+K^-$ process is reweighted by R_{FSR} . The data set at $\sqrt{s} = 3.65$ GeV with integrated luminosity 401 pb $^{-1}$ is utilized to study potential backgrounds from the continuum production, which is found to be negligible.

IV. DETERMINATION OF BRANCHING FRACTIONS

To obtain the signal yields, an unbinned maximum likelihood fit is performed to the invariant mass of $p\bar{p}K^+K^-$ from the 3C kinematic fit ($M_{p\bar{p}K^+K^-}^{3C}$). The full probability density function (PDF) is the incoherent sum of three components for the $\eta_c(2S)$ signal, the χ_{cJ} signal, and the $\psi(3686) \rightarrow p\bar{p}K^+K^-$ background. The

PDF of the $\eta_c(2S)$ signal is described as

$$\frac{d\Gamma}{dM} \epsilon(M) \otimes F_{\text{res}}^{(a)}(\delta m_1, \sigma_1) \otimes F_{\text{res}}^{(b)}(\delta m_2, \sigma_2), \quad (5)$$

Here, ϵ is the energy-dependent efficiency obtained by applying the Gaussian Process Regression (GPR) [34] to the discrete distribution of the efficiency extracted from the exclusive MC sample of the $\eta_c(2S)$ signal. The differential decay width is given by

$$\frac{d\Gamma}{dM} = \frac{2M^2}{\pi} \frac{E_\gamma^3 \mathcal{F}(E_\gamma) \Gamma^{\text{decay}}(M)}{(M^2 - m_{\eta_c(2S)}^2)^2 + m_{\eta_c(2S)}^2 \Gamma_{\eta_c(2S)}^2}. \quad (6)$$

where $2M^2/\pi$ is from the phase-space reduction, and $E_\gamma = (m_{\psi(3686)}^2 - M^2)/2m_{\psi(3686)}$ is the energy of the M1 photon in the rest frame of $\psi(3686)$. The empirical damping function $\mathcal{F}(E_\gamma)$ is adopted from the study of the KEDR experiment [35] and given by

$$\mathcal{F}(E_\gamma) = \frac{E_{\text{on}}^2}{E_\gamma E_{\text{on}} + (E_\gamma - E_{\text{on}})^2}, \quad (7)$$

where E_{on} is the energy of the photon calculated at the physical mass of $\eta_c(2S)$.

The Gaussian resolution functions $F_{\text{res}}^{(a)}$ and $F_{\text{res}}^{(b)}$ in Eq. 5 describe the resolution from simulation and the difference of resolution between the MC sample and data, respectively. The former is obtained from MC simulation, while the latter is fixed by linearly extrapolating δm_2 and σ_2 from the corresponding values of χ_{cJ} . The Γ^{decay} term in Eq. 6 represents the energy-dependent decay width of $\eta_c(2S) \rightarrow p\bar{p}K^+K^-$. Its lineshape is assumed to follow the phase space distribution. A signal MC sample of $\psi(3686) \rightarrow \gamma p\bar{p}K^+K^-$ with 0.5 million events is generated by the phase-space model. Then the GPR method is used to infer the actual Γ^{decay} function from the discrete mass distribution of the MC truth. The differential width $d\Gamma/dM$ after the GPR is related to Γ^{decay} by

$$\frac{d\Gamma}{dM} \sim \frac{2M^2}{\pi} E_\gamma(M) \Gamma^{\text{decay}}. \quad (8)$$

The freedom of choosing Γ^{decay} seems to be unavoidable before we know branching fractions of all intermediate decay modes, which is only achievable with much larger statistics but not possible in this study.

The invariant mass distributions from the exclusive MC samples of $\psi(3686) \rightarrow \gamma \chi_{cJ} \rightarrow \gamma p\bar{p}K^+K^-$ are used to model the shapes of the χ_{cJ} signal. The decays of χ_{cJ} are assumed to have uniform probability throughout the phase space. Furthermore, to account for the energy dependence in the E1-transition vertex, the PDFs of the χ_{cJ} signals are weighted event by event using the function w , given by

$$w = \left(\frac{E_\gamma(M_t)}{E_{\text{on}}} \right)^3 \times \mathcal{F}(E_\gamma(M_t)), \quad (9)$$

where M_t is the invariant mass of $p\bar{p}K^+K^-$ from the MC truth. The form of damping function is the same as Eq. (7), except that E_γ is calculated from the physical mass and E_{on} is replaced by the energy of the photon recoiling against on-shell χ_{cJ} . These PDFs are convolved with Gaussian functions to account for the resolution differences between the data and MC simulation. Due to the low background of this mode, the mass shift and resolution in the single Gaussians can be obtained by fitting the $M_{p\bar{p}K^+K^-}^{3C}$ distribution of data around the peaks of χ_{cJ} , and they are fixed in the final fit using full PDF.

The PDF of $\psi(3686) \rightarrow p\bar{p}K^+K^-$ is constructed using the exclusive MC sample of the $\psi(3686) \rightarrow p\bar{p}K^+K^-$ process, corrected by R_{FSR} , and convolved with a single Gaussian with floating mass shift and resolution.

In the default fit, the mass and width of the $\eta_c(2S)$ are fixed to their known values [17]. As a cross check, we also perform a fit with floating masses and widths and obtain values that are consistent with the known mass and width of $\eta_c(2S)$ within statistical uncertainties. An input-output check is performed, confirming the consistency between the output yields of $\eta_c(2S)$ and χ_{cJ} and the corresponding inputs.

The $M_{p\bar{p}K^+K^-}^{3C}$ distribution and the fit is shown in Fig. 1. Table I shows the signal yields of the $\eta_c(2S)$ and χ_{cJ} decays. The statistical significance of $\eta_c(2S)$ is 3.7σ , calculated by $\sqrt{-2 \ln(\mathcal{L}/\mathcal{L}_{\text{max}})}$, where \mathcal{L}_{max} and \mathcal{L} are the likelihoods with and without the signal of $\eta_c(2S)$, respectively. The product branching fractions shown in the last column of Table I are calculated using

$$\mathcal{B}[\psi(3686) \rightarrow \gamma X \rightarrow \gamma p\bar{p}K^+K^-] = \frac{N_X}{N_{\psi(3686)}^{\text{tot}} \epsilon_X}, \quad (10)$$

where N_X is the fitted yields of state $X \in \{\chi_{cJ}, \eta_c(2S)\}$, ϵ_X is the detection efficiency and $N_{\psi(3686)}^{\text{tot}} = (2712.4 \pm 14.3) \times 10^6$ is the number of $\psi(3686)$ events in data [18].

V. SYSTEMATIC UNCERTAINTIES

The systematic uncertainties are categorized into two types, i.e. the additive and the multiplicative uncertainties. These uncertainties are listed in Table II, and the details are discussed below.

A. The multiplicative uncertainties

The uncertainties of the tracking and PID of proton and kaon are studied in Refs. [36, 37] using $e^+e^- \rightarrow p\bar{p}\pi^+\pi^-$ and $e^+e^- \rightarrow \pi^+\pi^-K^+K^-$ as control samples, and the relative uncertainties of tracking and PID for both particles are estimated to be 1% per track.

The uncertainty associated with the reconstruction of photons is investigated using control samples of $J/\psi \rightarrow \rho^0\pi^0$ and $e^+e^- \rightarrow 2\gamma$ [38], from which the uncertainty in photon reconstruction is estimated to be 1% per photon.

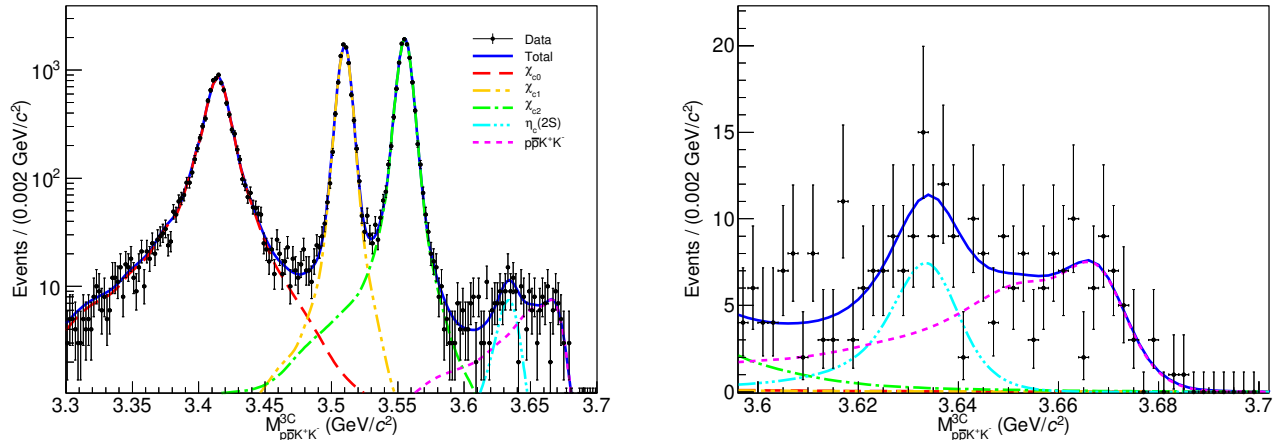


FIG. 1. The $M_{pp\bar{K}^+K^-}^{3C}$ distribution after the 3C kinematic fit. The points with error bars are data, and the blue solid, red long-dashed, yellow dash-dot-dotted, green dash-dotted and cyan dash-dot-dot-dotted lines represent the full PDF, PDFs of χ_{c0} , χ_{c1} , χ_{c2} and $\eta_c(2S)$, respectively. The purple short-dashed line is from the $\psi(3686) \rightarrow p\bar{p}K^+K^-$ background. The fit result in the signal region of $\eta_c(2S)$ is displayed in the right panel.

TABLE I. The measured branching fractions of $\psi(3686) \rightarrow \gamma\eta_c(2S) \rightarrow \gamma p\bar{p}K^+K^-$ and $\psi(3686) \rightarrow \gamma\chi_{cJ} \rightarrow \gamma p\bar{p}K^+K^-$. In the second column are signal yields with statistical uncertainties.

Mode	N_X	Branching fraction
$\psi(3686) \rightarrow \gamma\eta_c(2S) \rightarrow \gamma p\bar{p}K^+K^-$	84 ± 17	$(1.98 \pm 0.41 \pm 0.99) \times 10^{-7}$
$\psi(3686) \rightarrow \gamma\chi_{c0} \rightarrow \gamma p\bar{p}K^+K^-$	9952 ± 101	$(2.49 \pm 0.03 \pm 0.15) \times 10^{-5}$
$\psi(3686) \rightarrow \gamma\chi_{c1} \rightarrow \gamma p\bar{p}K^+K^-$	8721 ± 95	$(1.83 \pm 0.02 \pm 0.11) \times 10^{-5}$
$\psi(3686) \rightarrow \gamma\chi_{c2} \rightarrow \gamma p\bar{p}K^+K^-$	11463 ± 108	$(2.43 \pm 0.02 \pm 0.15) \times 10^{-5}$

Another study of $e^+e^- \rightarrow \gamma\mu^+\mu^-$ [39] process using J/ψ and $\psi(3770)$ data taken during 2009-2012 also shows this systematic uncertainty to be 1% at most. Applying the same method to 9 billion J/ψ events collected in 2009, 2018 and 2019, the uncertainty in the photon reconstruction efficiency is evaluated to be 0.5% for photons with energy in the range of [0.1,0.2] GeV. Since this corresponds to the energy range of photons recoiling against the χ_{cJ} states, the photon reconstruction uncertainty of 0.5% is adopted for the χ_{cJ} states and 1% for the photons recoiling against $\eta_c(2S)$, which have lower energy.

The uncertainty from the sampling of fake photons is estimated through varying the ratio r in each bin by $\pm 1\sigma$ around its nominal value, and the maximum difference in the efficiency is taken as the systematic uncertainty.

In the kinematic fit, the corrected helix parameters are used in the nominal result. To quantify the uncertainty associated with the helix parameter correction, half of the difference in efficiency with and without the helix parameter correction is taken as the systematic uncertainty.

The uncertainty in the total number of $\psi(3686)$ events, determined with inclusive hadronic $\psi(3686)$ decays, is 0.5% [18]. The uncertainty from the quoted branching fractions results from $\mathcal{B}[\chi_{cJ} \rightarrow I \rightarrow p\bar{p}K^+K^-]$ for different intermediate states I .

The value of α in the angular distribution of the pho-

ton in $\psi(3686) \rightarrow \gamma\chi_{cJ}$ depends on the transition dynamics. Although these processes are dominated by E1 transitions, a small fraction of the amplitude comes from M2 and E3 for χ_{c1} and χ_{c2} , as measured in Ref. [40]. MC samples are generated accordingly using the measured values from Ref. [40]. The difference in efficiency is taken as the systematic uncertainty..

B. The additive uncertainties

The primary background for the $\eta_c(2S)$ signal arises from the FSR process, which is sensitive to the value of the FSR correction factor. To assess the uncertainty from the lineshape of the background, the FSR factor is varied by $\pm 1\sigma$. The largest deviation in the fitted signal yield is then considered as the systematic uncertainty.

To estimate the uncertainty associated with non-resonant contributions, a first-order polynomial is added in the fit procedure. The resulting fit shows negligible polynomial background. The change in the log likelihood after the inclusion of the polynomial contribution is less than 0.001. Therefore, the polynomial background is ignored in the nominal result, which improves the stability of the fit. The difference in the signal yields with and without the polynomial is taken as the systematic

uncertainty.

The damping function is changed to $\exp(-E_\gamma^2/(8\beta^2))$, which was used by CLEO [41] assuming this form factor to depict the dynamics of the production vertex from $\psi(3686)$. The value of β is fixed at $\beta = 0.12$ GeV, which is obtained from the fit result of $\chi_{cJ} \rightarrow 2(\pi^+\pi^-)$ and $\eta_c(2S) \rightarrow 2(\pi^+\pi^-)$ in $\psi(3686) \rightarrow \gamma\chi_{cJ}$ and $\psi(3686) \rightarrow \gamma\eta_c(2S)$. The difference between the fitted signal yields are taken as the systematic uncertainty due to the damping function.

In this analysis, the fitting range is from 3.3 GeV to 3.7 GeV. The Barlow test [42] is performed to test the consistency of fitted signal yields in different fit ranges. The relative uncertainty for the branching fraction of the χ_{c0} signal is 0.12%, while no systematic uncertainty is assigned for other states.

To estimate the systematic uncertainty arising from the efficiency curve, one hundred samples of the efficiency curves are generated using the covariance and mean function of the GPR model. The samples of discrete points are interpolated linearly to replace the nominal efficiency curves. The distribution of events obtained using these alternative interpolated curves are fitted with a normal distribution, whose standard deviation is taken as the systematic uncertainty.

The difference between the MC simulation and the data is characterized by the mass shift δm_2 and the resolution σ_2 . The $\delta m_2(\sigma_2)$ of $\eta_c(2S)$ is estimated by fitting the $\delta m_2(\sigma_2)$ of χ_{cJ} with a first-order polynomial and extrapolate to the mass of $\eta_c(2S)$. The uncertainty of σ_2 arising from this linear assumption is estimated by comparing the nominal result with the one with increasing σ_2 by one standard deviation. To estimate the uncertainty of δm_2 , its value is varied by one standard deviation in both directions, and the larger difference in the fitted signal yields of $\eta_c(2S)$ is taken as the systematic uncertainty. Since δm_2 and σ_2 of $\eta_c(2S)$ are strongly positively correlated, the total systematic uncertainty is obtained by adding numbers from these two sources linearly.

VI. RESULTS AND DISCUSSION

The measured branching fractions are shown in Table I. The significance of the $\eta_c(2S)$ signal is 3.3σ after considering the systematic uncertainty. To obtain a conservative estimation for the upper limit of $\mathcal{B}[\psi(3686) \rightarrow \gamma\eta_c(2S) \rightarrow \gamma p\bar{p}K^+K^-]$, the FSR factor R_{FSR} is set to a value one standard deviation lower than the nominal one, and the CLEO form factor with $\beta = 0.12$ GeV is used. The curve of likelihood, as a function of N , is then convolved with a single Gaussian via the following formula:

$$\tilde{L}(N) = \int_0^1 L\left(\frac{\epsilon}{\hat{\epsilon}}N\right) \frac{1}{\sqrt{2\pi\sigma_\epsilon^2}} e^{-\frac{(\epsilon-\hat{\epsilon})^2}{2\sigma_\epsilon^2}} d\epsilon. \quad (11)$$

Here, $\hat{\epsilon}$ represents the nominal efficiency, and σ_ϵ denotes the multiplicative systematic uncertainty associ-

ated with it. The upper limit of $\mathcal{B}[\psi(3686) \rightarrow \gamma\eta_c(2S) \rightarrow \gamma p\bar{p}K^+K^-]$ at 90% C.L. is set to be 4.1×10^{-7} .

Since the product branching fractions of $\psi(3686) \rightarrow \gamma\chi_{cJ} \rightarrow \gamma p\bar{p}K^+K^-$ were not reported in the previous study using 106 million $\psi(3686)$ events [19], the branching fractions of $\mathcal{B}[\chi_{cJ} \rightarrow p\bar{p}K^+K^-]$ are estimated by incoherently summing the measured branching fractions shown in Table III. To estimate the uncertainty of the incoherent sum, the branching fractions in Table III are assumed to be independent on each other. In the calculation, $\mathcal{B}[\Lambda(1520) \rightarrow pK^-] = 0.23 \pm (0.01 \times 0.23/0.45)$ is assumed, where the 0.45 is the branching fraction of $\Lambda(1520) \rightarrow N\bar{K}$ from the PDG [17]. For $\phi \rightarrow K^+K^-$, $\mathcal{B}[\phi \rightarrow K^+K^-] = 0.491 \pm 0.001$ is adopted. For values with upper limit only, the measured value is treated to be zero and the upper limit is taken as the uncertainty. The results are shown in Table IV, where the branching fractions calculated from this work together with the branching fractions of $\psi(3686) \rightarrow \gamma\chi_{cJ}$ are also listed. All branching fractions are assumed to be independent on each other. The branching fractions from this work agree with those in Ref. [19], while the precision is improved. Given the current large statistics, a partial wave analysis is necessary to obtain more reliable measurements of the branching fractions of these decay modes of χ_{cJ} , which is beyond the scope of this paper. Nevertheless, the previous measurement can be considered as a rough estimation and is complementary to the measurement of product branching fractions in this work.

VII. SUMMARY

In summary, based on $(2712.4 \pm 14.3) \times 10^6$ $\psi(3686)$ events collected with the BESIII detector at BEPCII, the branching fractions of $\psi(3686) \rightarrow \gamma\eta_c(2S)$, $\gamma\chi_{cJ} \rightarrow \gamma p\bar{p}K^+K^-$ are measured. The first evidence for the $\eta_c(2S)$ in this mode is found with a significance of 3.3σ after considering the systematic uncertainties. The branching fraction of $\psi(3686) \rightarrow \gamma\eta_c(2S) \rightarrow \gamma p\bar{p}K^+K^-$ is measured to be $(1.98 \pm 0.41 \pm 0.99) \times 10^{-7}$, and its upper limit at 90% C.L. is set to be 4.1×10^{-7} . The branching fractions of $\psi(3686) \rightarrow \gamma\chi_{cJ} \rightarrow \gamma p\bar{p}K^+K^-$ are determined to be $(2.49 \pm 0.03 \pm 0.15) \times 10^{-5}$, $(1.83 \pm 0.02 \pm 0.11) \times 10^{-5}$, and $(2.43 \pm 0.02 \pm 0.15) \times 10^{-5}$, for χ_{c0} , χ_{c1} , and χ_{c2} , respectively. Benefiting from the high statistics of χ_{cJ} and negligible background, these decay modes hold great promise to achieve a deeper understanding of their decay dynamics, especially the baryons and light mesons interactions, in further studies.

ACKNOWLEDGMENTS

The BESIII Collaboration thanks the staff of BEPCII and the IHEP computing center for their strong support. This work is supported in part by National Key R&D Program of China under Contracts Nos.

TABLE II. Systematic uncertainties in product branching fractions. The total uncertainty is taken as the sum of all terms in quadrature.

Item	$\eta_c(2S)$	χ_{c0}	χ_{c1}	χ_{c2}
Tracking	4.0%	4.0%	4.0%	4.0%
PID	4.0%	4.0%	4.0%	4.0%
Photon reconstruction	1.0%	0.5%	0.5%	0.5%
Photon sampling	0.8%	0.2%	1.3%	1.3%
Kinematic fit	2.1%	1.6%	1.8%	1.9%
$N_{\psi(3686)}$	0.5%	0.5%	0.5%	0.5%
\mathcal{B} from PDG	-	0.4%	0.5%	0.5%
α	-	-	0.1%	0.9%
FSR	16%	-	-	0.1%
Background shape	0.2%	-	-	-
Damping function	47%	0.1%	0.1%	0.1%
Fit range	-	0.1%	-	-
Efficiency curve	0.5%	-	-	-
Resolution	1.4%	-	-	-
Total	50%	6.0%	6.2%	6.2%

TABLE III. The branching fractions of $\chi_{cJ} \rightarrow p\bar{p}K^+K^-$ through different modes measured before this work [17].

State	non-resonant	$\Lambda(1520)\bar{\Lambda}(1520)$	$K^+\bar{p}\Lambda(1520) + \text{c.c.}$	$p\bar{p}\phi$
χ_{c0}	$(1.2 \pm 0.3) \times 10^{-4}$	$(3.1 \pm 1.2) \times 10^{-4}$	$(3.0 \pm 0.8) \times 10^{-4}$	$(6.0 \pm 1.4) \times 10^{-5}$
χ_{c1}	$(1.3 \pm 0.2) \times 10^{-4}$	$< 9 \times 10^{-5}$	$(1.7 \pm 0.4) \times 10^{-4}$	$< 1.7 \times 10^{-5}$
χ_{c2}	$(1.9 \pm 0.3) \times 10^{-4}$	$(4.7 \pm 1.5) \times 10^{-4}$	$(2.9 \pm 0.7) \times 10^{-4}$	$(2.8 \pm 0.9) \times 10^{-5}$

2020YFA0406300, 2020YFA0406400, 2023YFA1606000; National Natural Science Foundation of China (NSFC) under Contracts Nos. 11635010, 11735014, 11935015, 11935016, 11935018, 12025502, 12035009, 12035013, 12061131003, 12192260, 12192261, 12192262, 12192263, 12192264, 12192265, 12221005, 12225509, 12235017, 12361141819; the Chinese Academy of Sciences (CAS) Large-Scale Scientific Facility Program; the CAS Center for Excellence in Particle Physics (CCEPP); Joint Large-Scale Scientific Facility Funds of the NSFC and CAS under Contract No. U1832207; 100 Talents Program of CAS; The Institute of Nuclear and Particle Physics (INPAC) and Shanghai Key Laboratory for Particle Physics and Cosmology; German Research Foundation DFG under Contracts Nos. FOR5327, GRK 2149; Istituto Nazionale di Fisica Nucleare, Italy; Knut and Alice Wallenberg Foundation under Contracts Nos. 2021.0174, 2021.0299; Ministry of Development of Turkey under Contract No. DPT2006K-120470; National Research Foundation of Korea under Contract No. NRF-2022R1A2C1092335; National Science and Technology fund of Mongolia; National Science Research and Innovation Fund (NSRF) via the Program Management Unit for Human Resources & Institutional Development, Re-

search and Innovation of Thailand under Contracts Nos. B16F640076, B50G670107; Polish National Science Centre under Contract No. 2019/35/O/ST2/02907; Swedish Research Council under Contract No. 2019.04595; The Swedish Foundation for International Cooperation in Research and Higher Education under Contract No. CH2018-7756; U. S. Department of Energy under Contract No. DE-FG02-05ER41374

TABLE IV. The branching fractions of $\chi_{cJ} \rightarrow p\bar{p}K^+K^-$ from Ref. [19] and this work. The branching fractions of $\psi(3686) \rightarrow \gamma\chi_{cJ}$ are quoted from PDG [17]. The uncertainties are combined.

State	$\mathcal{B}[\psi(3686) \rightarrow \gamma\chi_{cJ}]$	Ref. [19]	This work
χ_{c0}	$(9.77 \pm 0.23)\%$	$(2.3 \pm 0.3) \times 10^{-4}$	$(2.55 \pm 0.17) \times 10^{-4}$
χ_{c1}	$(9.75 \pm 0.27)\%$	$(1.7 \pm 0.3) \times 10^{-4}$	$(1.87 \pm 0.13) \times 10^{-4}$
χ_{c2}	$(9.36 \pm 0.23)\%$	$(2.9 \pm 0.6) \times 10^{-4}$	$(2.59 \pm 0.17) \times 10^{-4}$

-
- [1] X. H. Mo, C. Z. Yuan and P. Wang, *HEPNP* **31**, 686 (2007).
- [2] T. Appelquist and H. D. Politzer, *Phys. Rev. Lett.* **34**, 43 (1975).
- [3] M. E. B. Franklin, G. J. Feldman, G. S. Abrams, M. S. Alam, C. A. Blocker, A. Blondel, A. Boyarski, M. Breidenbach, D. L. Burke and W. C. Carithers *et al.* *Phys. Rev. Lett.* **51**, 963 (1983).
- [4] M. Anselmino, M. Genovese and E. Predazzi, *Phys. Rev. D* **44**, 1597 (1991).
- [5] K. T. Chao, Y. F. Gu and S. F. Tuan, *Commun. Theor. Phys.* **25**, 471 (1996).
- [6] H. Wang and C. Z. Yuan, *Chin. Phys. C* **46**, 071001 (2022).
- [7] S. K. Choi *et al.* [Belle], *Phys. Rev. Lett.* **89**, 102001 (2002).
- [8] B. Aubert *et al.* [BaBar], *Phys. Rev. Lett.* **92**, 142002 (2004).
- [9] D. M. Asner *et al.* [CLEO], *Phys. Rev. Lett.* **92**, 142001 (2004).
- [10] P. del Amo Sanchez *et al.* [BaBar], *Phys. Rev. D* **84**, 012004 (2011).
- [11] T. Barnes, S. Godfrey and E. S. Swanson, *Phys. Rev. D* **72**, 054026 (2005).
- [12] G. Li and Q. Zhao, *Phys. Lett. B* **670**, 55 (2008).
- [13] T. Peng and B. Q. Ma, *Eur. Phys. J. A* **48**, 66 (2012).
- [14] G. Li and Q. Zhao, *Phys. Rev. D* **84**, 074005 (2011).
- [15] H. Negash and S. Bhatnagar, *Adv. High Energy Phys.* **2017**, 7306825 (2017).
- [16] M. Ablikim *et al.* [BES], *Phys. Rev. Lett.* **109**, 042003 (2012).
- [17] S. Navas *et al.* [Particle Data Group], *Phys. Rev. D* **110**, 030001 (2024).
- [18] M. Ablikim *et al.* [BESIII], [arXiv:2403.06766 [hep-ex]].
- [19] M. Ablikim *et al.* [BESIII], *Phys. Rev. D* **83**, 112009 (2011).
- [20] M. Ablikim *et al.* [BESIII], *Nucl. Instrum. Meth. A* **614**, 345 (2010).
- [21] X. Li, Y. Sun, C. Li, Z. Liu, Y. Heng, M. Shao, X. Wang, Z. Wu, P. Cao and M. Chen *et al.* *Radiat. Detect. Technol. Methods* **1**, 13 (2017).
- [22] Y. X. Guo, S. S. Sun, F. F. An, R. X. Yang, M. Zhou, Z. Wu, H. L. Dai, Y. K. Heng, C. Li and Z. Y. Deng *et al.* *Radiat. Detect. Technol. Methods* **1**, 15 (2017).
- [23] P. Cao, H. F. Chen, M. M. Chen, H. L. Dai, Y. K. Heng, X. L. Ji, X. S. Jiang, C. Li, X. Li and S. B. Liu *et al.* *Nucl. Instrum. Meth. A* **953**, 163053 (2020).
- [24] S. Agostinelli *et al.* [GEANT4], *Nucl. Instrum. Meth. A* **506**, 250 (2003).
- [25] Z. Y. Deng, G. F. Cao *et al.*, *Chin. Phys. C* **30**, 371 (2006).
- [26] S. Jadach, B. F. L. Ward and Z. Was, *Phys. Rev. D* **63**, 113009 (2001).
- [27] S. Jadach, B. F. L. Ward and Z. Was, *Comput. Phys. Commun.* **130**, 260 (2000).
- [28] D. J. Lange, *Nucl. Instrum. Meth. A* **462**, 152 (2001).
- [29] R. G. Ping, *Chin. Phys. C* **32**, 599 (2008).
- [30] E. Richter-Was, *Phys. Lett. B* **303**, 163 (1993).
- [31] M. Ablikim *et al.* [BES], *Phys. Rev. D* **70**, 092004 (2004).
- [32] X. Zhou, S. Du, G. Li and C. Shen, *Comput. Phys. Commun.* **258**, 107540 (2021).
- [33] G. Punzi, eConf **C030908**, MODT002 (2003). [arXiv:physics/0308063 [physics]].
- [34] C. E. Rasmussen and C. K. I. Williams, *The MIT Press, Cambridge, MA, USA, 2006*, ISBN: 026218253X.
- [35] V. V. Anashin, V. M. Aulchenko, E. M. Baldin, A. K. Barladyan, A. Y. Barnyakov, M. Y. Barnyakov, S. E. Baru, I. Y. Basok, I. V. Bedny and O. L. Beloborodova *et al.* *Int. J. Mod. Phys. Conf. Ser.* **02**, 188 (2011).
- [36] M. Ablikim *et al.* [BESIII], *Phys. Rev. Lett.* **124**, 042001 (2020).
- [37] M. Ablikim *et al.* [BESIII], *Phys. Rev. D* **109**, 032004 (2024).
- [38] M. Ablikim *et al.* [BESIII], *Phys. Rev. D* **81**, 052005 (2010).
- [39] V. Prasad, C. Liu, X. Ji, W. Li, H. Liu and X. Lou, *Springer Proc. Phys.* **174**, 577 (2016).
- [40] M. Ablikim *et al.* [BESIII], *Phys. Rev. D* **95**, 072004 (2017).
- [41] R. E. Mitchell *et al.* [CLEO], *Phys. Rev. Lett.* **102**, 011801 (2009). [erratum: *Phys. Rev. Lett.* **106**, 159903 (2011)].
- [42] R. Barlow, [arXiv:hep-ex/0207026 [hep-ex]].